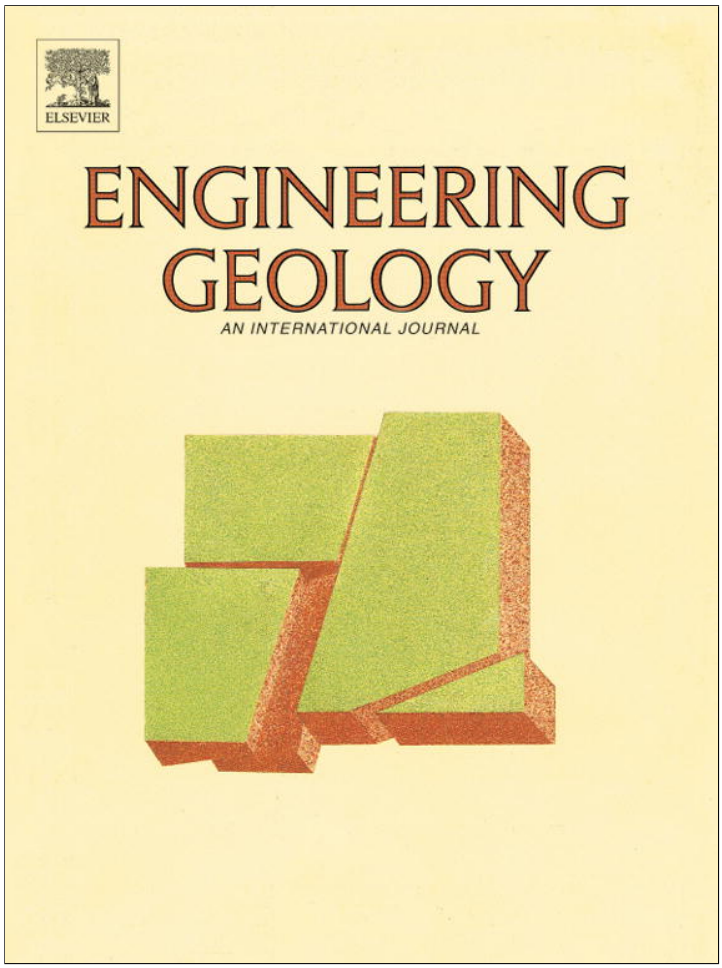

(This is a sample cover image for this issue. The actual cover is not yet available at this time.)

Engineering Geology 154 (2013) 131–141

Contents lists available at SciVerse ScienceDirect

Engineering Geology

journal homepage: www.elsevier.com/locate/enggeo

An experimental study on the influence of surface finishing on the weathering of a building low-porous limestone in coastal environments

Maja Urosevic *, Eduardo Sebastián, Carolina Cardell

Department of Mineralogy and Petrology, Faculty of Science, University of Granada, Campus Fuentenueva s/n, 18071 Granada, Spain

ARTICLE INFO

Article history:
Received 18 July 2011
Received in revised form 20 December 2012
Accepted 29 December 2012
Available online 10 January 2013

Keywords:
Salt spray damage
Low-porous limestone
Coastal environment
Ageing test
Gypsum
Halite

ABSTRACT

Limestones used as building material are especially prone to weathering in coastal environments due to interactions between sea mist and the carbonate stone. Subtle variations of the commercial surface finishing may lead to differences in decay patterns and aesthetic properties due to salt crystallization. To explore this potentially contrasting behavior, tablets of rough and polished low-porous limestone were aged in a sea-salt spray corrosion chamber to simulate their exposure in a coastal environment. Different crystallization morphologies and relative proportions of soluble (halite) and less soluble (gypsum) salts were observed in the aged rough and polished surface samples. These morphologies are ascribed to the microtextural characteristics and the surface pore systems of the diverse (rough and polished) substrates that in turn influence fluid (saline solution) transport toward their interior, as well as the different salt solubilities interacting with the substrates. Polished surfaces exhibit little evidence of damage after the ageing test in contrast to the rough samples but do have conspicuous gypsum on the surface together with halite. The scarcity of gypsum on the rough surfaces, in addition to a more severe change in the porosity system, suggests that salts penetrate deeper when the stone surface is not polished. Potential decay induced by salt crystallization pressure is therefore minimized when the stone surface is polished. However, polished surfaces show more significant changes in luminosity and chroma after the ageing test, and so are less attractive from an aesthetic point of view. Surface finishing is thus an important feature that needs to be characterized for a better understanding of the weathering behavior of building stones used in coastal environments.

1. Introduction

It has long been recognized that limestones (carbonate rocks composed largely of the mineral calcite, $CaCO_3$) exposed to outdoor environments are more prone to weathering than other stone lithotypes such as sandstones or granites (Cardell et al., 2003a; Smith et al., 2010). This is mainly due to water deposition at the limestone surface that acts as a solvent for a series of gaseous substances present in the atmosphere, as well as air pollutants that are very reactive in contact with carbonate minerals (e.g. Thornbush and Viles, 2007). Among other regimes, marine environments are especially aggressive to building stone materials including granites (e.g. Rivas et al., 2010) and carbonates (Birginie et al., 2000; Zendri et al., 2000, 2001; Cardell et al., 2003a,b; Silva and Simão, 2009) because dissolution-precipitation processes are thought to be accelerated by the presence of marine aerosols that can include very reactive sulfate solutions (Zezza and Macrì, 1995; Theoulakis and Moropoulou, 1999; Cardell et al., 2003a,b, 2008; Angeli et al., 2010; Ruiz-Agudo et al., 2007, 2011). Although in low quantities, marine aerosols may also be transported by winds to inland areas relatively far from the coast (e.g. Zezza and Macrì, 1995; Silva et al., 2007; Meira et al., 2008; Anwar Hossain et al., 2009; Horemans et al., 2011; Kontozova-Deutsch et al., 2011; Urosevic et al., 2012) and have been also found in arid regions (Zaouia et al., 2005) making this issue an important research area to influence future conservation strategies in inland areas.

Pioneering works on the morphological variations of limestone surface under marine environment have stressed a limited weathering effect of condensed water (Zendri et al., 2000, 2001). Observations in natural environments, however, suggest that other wet deposition mechanisms must prevail as a large variety of weathering forms in limestone have been described in coastal environments (Zezza and Macrì, 1995; Chabas et al., 2000; Cardell et al., 2003a,b; Smith et al., 2010). More likely wet surface deposition is produced directly by sea spray (Cardell et al., 2003a,b; Silva and Simão, 2009) instead of direct water condensation, as the latter is formed only near 100% relative humidity. Nevertheless, direct condensation of moisture onto cold surfaces (i.e. when the monument temperature is below the dew point) is also very common in coastal areas, where sea spray causes condensation at RH = 75%, as reported by Del Monte and Rossi (1997). Additionally marine aerosol dry deposition must be considered (Stefanis et al., 2009). Furthermore the combination of salts and the heterogeneous distribution of wind flow in coastal environment eventually control the surface decay pattern (Rodriguez-Navarro et al., 1999).

* Corresponding author. Tel.: +34 958246614; fax: +34 958243368.
E-mail address: maja@ugr.es (M. Urosevic).

0013-7952/$ – see front matter © 2013 Elsevier B.V. All rights reserved.
http://dx.doi.org/10.1016/j.enggeo.2012.12.013

Recently it has been shown that different surface finishing processes may potentially control contrasting stone decay behavior in porous materials (Urosevic et al., 2010). Moreover, different hydrophilicities at the surface may induce changes in the system evaporation rate and hence modify the precipitation/dissolution cycles of soluble salts resulting in different salt crust morphologies on the stone surface (Zendri et al., 2000; Cardell et al., 2003b). It is well established that the morphology and mineralogy of the weathering crusts are strongly influenced by local microclimatic conditions which result in contrasting scaling patterns due to salt-induced decay (Cardell et al., 2003a; Smith et al., 2003; Török, 2003; Török and Rozgonyi, 2004; Urosevic et al., 2012). In addition to the microclimatic environment such as humidity, temperature and wind, the surface roughness should also be considered as an important factor as it potentially can change the nature and morphology of the crystallizing mineral phases under the same substrate (Urosevic et al., 2010). Nevertheless the implications of surface finishings for the weathering of limestones under marine environments have not been considered so far.

This work presents a laboratory ageing test using marine spray in a controlled atmosphere chamber (Birginie et al., 2000; Cardell et al., 2003b; Rivas et al., 2003; Urosevic et al., 2010) to examine the weathering decay in low-porous rough and polished limestone samples. This work is aimed to explore different deterioration behaviors due to contrasting finishing of stone surfaces as well as to characterize the condensed phases and their morphological variations.

2. Material and methods

2.1. Stone material

This research focuses on a low-porous Jurassic limestone known as Sierra Elvira stone (SE). This limestone is currently used as a building stone extracted in Andalusia (Granada province, Southern Spain). A similar stone variety in age and geological depositional environment is found in many other Alpine ranges and is extensively used throughout Europe. The sawing direction of the selected material is perpendicular to the layering (vein cut). This layering is due to a thin alternation of parallel- to cross-laminated beds that has been interpreted as storm sand layers (Dabrio and Polo, 1985). Two finishing surface types of the SE limestone are commercialized, named as rough surface and polished surface. The latter finishing type does not require any treatment before the polishing process because of its high strength. In this work, limestone samples with rough and polished surfaces were cut as tablet samples ($50\times50\times10$ mm) for the sea-salt spray ageing test. Then the stone samples were prepared according to the requirement of each analytical technique applied, as specified in Section 2.3 (Figures 1a and b).

The SE limestone is a medium-grain limestone mainly composed of well cemented carbonate bioclastic fragments of crinoids (equinoderms). It is by far the most exploited stone variety in the Granada area and widely used for ornamental purposes in historical monuments and in modern buildings in Spain (Sebastián Pardo et al., 2008). The SE limestone is classified by means of optical microscopy as a biopelsparite (Ibp) according to Folk (1981), and is comprised chiefly of allochemical constituents (pellets and fragments of fossil equinoderms, molluscs, brachiopods and scarce foraminifera) cemented by sparry calcite cement (10–100 μm in size) as shown in Fig. 2. Crinoids (equinoderms) are the main allochemical constituents (50–70%), showing a diameter of 1–2 mm. Stylolites (fine lines, usually brownish in color, formed by pressure-solution) can be also present, but their proportions vary over two stratigraphic units exploited in the quarry of Sierra Elvira (Granada, Southern Spain). The lower level is characterized by large-scale unidirectional sedimentary lamination and a high density of stylolites whereas in the upper lever stylolites are less abundant. An important feature of this limestone is the occurrence of variable amounts of dolomite ($CaMg(CO_3)_2$) as a result of a non-homogeneous syn- to post-consolidation dolomitization process. The presence of dolomite generates a relatively high MgO content in the bulk composition (ca. 4 wt.%) when compared to other common limestones (Buj et al., 2010). The amount of dolomite in the studied limestone samples is ca. 18 wt.%, based on XRF data (Table 1).

2.2. Sea-salt ageing test

Six limestone tablets were subjected to a modified UNE-EN 14147 (1994) ageing test in a saline spray chamber (CCONS series, INELTEC®) to investigate the effect of marine aerosol deposition on the rough and polished stone surfaces. In order to re-create more realistic environmental conditions of coastal areas, seawater was collected from the Mediterranean Sea at Granada coast (Salobreña, Southern Spain). Stone tablets were hung vertically on a nylon thread from plastic bars inside the chamber and submitted to 160 cycles until no significant macroscopic changes were observed in the stones. Each cycle consisted of 3 h of seawater spray followed by 6 h of drying by forced air at 35 °C and relative humidity of 70 ± 2%. The chamber remained closed throughout the test, thus during spray periods the relative humidity was ca. 98%. The composition of the seawater is shown in Table 2. Cations (Ca^{2+}, K^{+}, Na^{+} and Mg^{2+}) were determined by means of inductively coupled plasma-atomic emission spectrometry (ICP-AES, Leeman Labs PS series) and anions (Cl^{-}, SO_4^{2-} and NO_3^{-}) by ion chromatography (IC, Dionex DX 300). The pH of the seawater was 7.84 at 20 °C (Eutech 1500). Macroscale observations and photographic records were made throughout the test to determine the presence of efflorescences, evolution of crystalline habits on the stone surfaces, drying and decay of the samples. Moreover, before and after the test the tablets were weighed. To further explore the influence of the substrate on the composition and habits of the precipitated salts, a blank crystallization test was conducted using glass as an impermeable substrate. The glass was placed inside the saline spray chamber and was subjected to the same experimental conditions and seawater as the limestone samples. Afterwards the nature and morphology of the crystallized efflorescences were analyzed by means of environmental scanning electron microscope.

2.3. Analytical techniques

The mineral composition of the SE limestone and the crystallized efflorescences were determined by X-ray powder diffraction (XRD) on a Philips PW-1710 diffractometer equipped with an automatic slit window. Samples were previously milled in an agate mortar to less than 50 μm particle size. Analysis conditions were: radiation Cu Kα (λ: 1.5405 Å), 40 kV voltage, 40 mA current intensity, explored area between 2θ 3°–60° and 2θ goniometer speed of 0.01° s^{-1}. Automatic acquisition, evaluation and identification of minerals were performed by the Xpowder software (Martín Ramos, 2004). Major and trace elements of fresh limestone were analyzed using a Bruker S4 Pioneer X-ray fluorescence spectrometer (XRF) with wavelength dispersion equipped with a goniometer that held analyzing crystals (LIF200/PET/OVO-55) and Rh X-ray tube (60 kV, 150 mA).

Polished thin sections of fresh and aged limestones were examined under polarizing optical microscopy (OM) using an Olympus BX-60 equipped with digital camera (Olympus DP10). The morphologies and composition of the mineral phases precipitated onto the rough and polished surfaces were investigated in depth using an environmental scanning microscope (ESEM) with Energy-Dispersive Spectroscopy (EDS). This technique enables the morphology characterization of delicate hydrous salts that are not stable under normal high vacuum conditions. A Phillips Quanta 400 microscope was used applying 20 kV acceleration voltage, 1 nA probe current and working distance of 10 mm.

The limestone pore system was characterized by means of mercury intrusion porosimetry (MIP) and argon adsorption. Blocks of ca. 2 cm^3 of fresh and aged samples (containing salts) were dried in an oven during 24 h at 60 °C, and analyzed on a Micromeritics Autopore III model

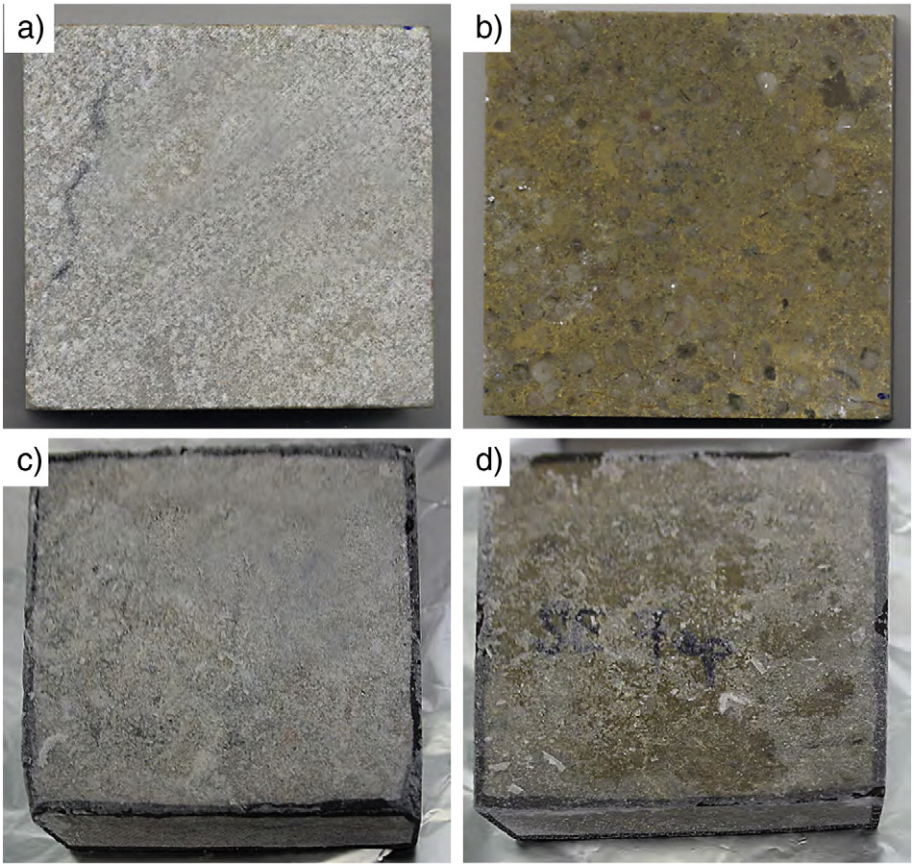

Fig. 1. Sierra Elvira limestone: (a) rough and (b) polished fresh surface before the test, (c) rough and (d) polished aged surface after the test. Tablets are 5cm in width.

9410 porosimeter. In addition, aged samples were washed in distilled water during one week after the ageing test, and studied by means of MIP and argon adsorption. The Barret–Joyner–Halenda (BJH) method was used to obtain the pore size distribution curves, the pore volume and the mean pore size of the limestone samples (Barrett et al., 1951).

Chromatic parameters of rough and polished stone surfaces were determined before and after the ageing test using a Minolta CR 210 colorimeter, with 0° viewing angle and 50 mm diameter measuring area. The CIE 1976 chromatic scale was used to measure the parameters L*, a* and b*. After the ageing test the following approach was applied: (1) measurements on surfaces covered by salt crusts and (2) measurements on surfaces where efflorescences were mechanically removed. The second approach can be useful to evaluate the efficiency of cleaning interventions to recuperate original stone chromatic characteristics.

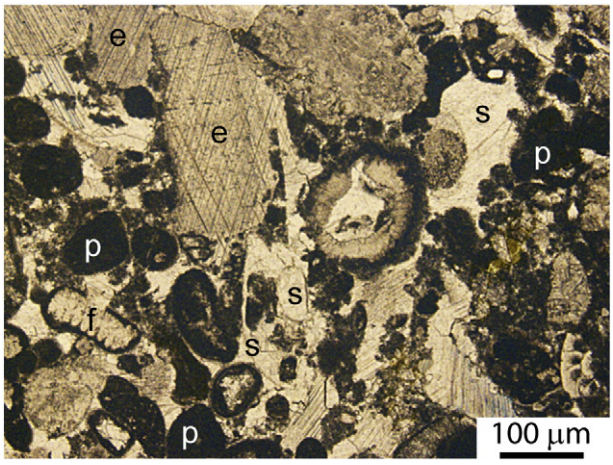

Fig. 2. Optical microphotograph showing a representative texture of fresh quarried Sierra Elvira low-porous limestone: fragments of equinoderms (e), pellets (p), and foraminera (f) cemented by sparry calcite (s). Transmitted light, parallel nicols.

3. Results

3.1. Macroscopic changes

During the sea-salt ageing test no stone detachments or scaling were observed. The first efflorescences crystallized in all samples as crusts after 48 h of exposure in the test chamber. Salt crusts started to grow at the upper borders of each tablet and afterwards extended and covered the tablets completely (Figure 1). A more continuous and evenly distributed crust was systematically found in the rough samples (Figure 1c). The weight of all samples slightly increased after the test (+0.25% for rough limestone and +0.40% for polished limestone). This is in agreement with other experimental results that suggest only very small and gradual changes in weight for silicate rocks and compact microcrystalline limestone, whereas in more porous materials scaling and disaggregation induced by sea-salt damage lead to a weight loss (Rivas et al., 2003; Silva and Simão, 2009). The salt crust was thicker in the polished limestones (ca. 0.5–1 mm) compared to the rough ones (<0.5 mm). Furthermore, thin sections prepared perpendicular to the limestone surfaces did not reveal the presence of subefflorescences although the occurrence of small amount of precipitated salts in the pore system near the surface for the rough samples was inferred based on the modification of the pore system after the ageing test (see Sections 3.3. and 4.2).

Table 1
Representative major bulk rock composition and trace elements of SE limestone (this study) together with mean values of Campanile limestone (Buj et al., 2010).

wt.%	Sierra Elvira	Campanile
SiO_2	0.52	0.51
TiO_2	0.01	b.d.l.
Al_2O_3	0.21	0.10
Fe_2O_3	0.18	0.09
MnO	0.01	0.10
MgO	4.22	0.86
CaO	50.66	54.54
Na_2O	0.03	0.15
K_2O	0.06	0.02
P_2O_5	0.02	0.03
SO_3	0.03	n.m.
Cl	0.02	n.m.
ppm		
Cu	41	n.m.
Zn	n.m.	n.m.
Sr	132	n.m.
Zr	7	n.m.

Detection limit is 0.005 wt.% for major elements and for trace elements 3 ppm for Zr, 2 ppm for Sr, 1 ppm for Cu, Zn, Zr.
b.d.l.: below detection limit, n.m.: not measured.

3.2. Nature and morphology of the crystallized mineral phases

A key finding of this study is the distinct nature and morphology of the salt crust precipitated onto the aged rough versus polished limestone surfaces and the glass crystallizer observed with ESEM. These morphologies are described separately in the following paragraphs.

3.2.1. Rough surface

A semi continuous, homogeneous and thin halite (NaCl) crust was developed onto the rough limestone surface (Figures 3a and b). The crust was 50–100 μm thick, relatively flat and with a smooth surface. The mineralogy of the crust was essentially constituted by halite although gypsum was occasionally detected representing less than ca. 2–5% of the crust by volume. Halite shows anhedral crystal shapes (no crystal face development). Under ESEM inspection some discontinuities were seen in the crust as shown in Fig. 3b. Here subhedral (poor crystal face development) and small (5–10 μm) halite crystals together with small amount of ferruginous clays usually occur. Chemical dissolution in the part of the surface not covered by the halite crust is not evident (Figure 3c).

3.2.2. Polished surface

Aged polished surfaces are characterized by higher diversity of crystalline habits and salt species. In contrast to the rough surface samples, the crust is thick and discontinuous; it mostly consists of clusters of large single halite crystals up to 100 μm in size, as observed in Fig. 3d and e. Halite occurs as subhedral to euhedral crystals (well developed crystal faces) growing with no crystallographic preferred orientation on the limestone surface. The {100} crystal forms are commonly parallel to the polished surface (Figures 3d and e).

Table 2
Sea-salt composition (expressed in ppm) used in the artificial ageing test of the present study and from Cardell et al., 2003b.

	This study	Cardell et al., 2003b
Cl^-	12,879	22,050
NO_3^-	72	50
SO_4^{2-}	2772	2713
Ca^{2+}	330	345
K^+	348.4	1020
Na^+	10,030	19,920
Mg^{2+}	1069	945
HPO_4^{2-}	Not measured	28

Although halite is again the main salt forming the crust, calcium sulfate is also conspicuously present (Figures 3e and f) and represents approximately 10–15 vol.% of the crust. While in this work the precise composition of the calcium sulfate could not be established with the applied analytical techniques, the experimental conditions of the test (98% RH and T = 35 °C) imply that gypsum ($CaSO_4 \cdot 2H_2O$) should be the stable phase (Charola et al., 2007; Kramar et al., 2010a), since at room temperature and relative humidity lower than 70% gypsum dehydrates to bassanite ($CaSO_4 \cdot 0.5H_2O$) and anhydrite ($CaSO_4$). Moreover, considering that the kinetics of these dehydration reactions are very slow (Charola et al., 2007; Kramar et al., 2010a) in the following discussion only gypsum will be considered. Gypsum distinctively occurs as small radial aggregates of multiple aciculae (slender or needle-like crystals) as can be observed in Fig. 3f. Gypsum needles seldom exceed 50 μm in length and 2–3 μm in width. This morphology clearly differs from that commonly reported in urban areas where gypsum crystallizes due to the dissolution of atmospheric SO_2 in polluted fog droplets. In the latter case gypsum usually occurs as clusters of "rosette" habits (Del Monte and Rossi, 1997; Simão et al., 2006). Gypsum needle morphologies such as those observed here have been also reported on granite surfaces subjected to a sea-salt ageing test (Cardell et al., 2003a). In our experiments, gypsum directly precipitated from the marine solution. Textural relationships between crystallized salts indicate that gypsum precipitated first and afterwards was overgrown by larger halite crystals.

3.2.3. Blank crystallization test

In the glass crystallizer the composition of the salts was more complex. Minerals found with ESEM/EDS analysis included halite, gypsum, silvine (KCl) and epsomite ($MgSO_4 \cdot 7H_2O$). As mentioned above, this technique does not permit identification of the sulfate species, however considering the experimental test conditions we infer that in fact gypsum and epsomite are the mineral phases present (Zehnder and Arnold, 1989). Regarding the observed salt morphologies, these were rather different from those previously described for rough and polished limestone surfaces. Relatively large gypsum crystals (>100 mm in length and 50 mm) that were typically twinned on {100} crystal planes were the most conspicuous morphology encountered. The twins were composed of two or four crystals with simple habit (tabular on {010} planes with edges beveled by {120} planes) resulting in swallowtail morphologies (Figure 4a). Gypsum twins were usually overgrown by halite. Large subhedral halite crystals (ca. 1 mm in size, Figure 4b) with typical hopper morphologies (crystal displaying an hourglass shape) were common whereas smaller (20–50 mm) and more euhedral halite crystals were associated with the twinned gypsum (Figure 4a). Small, non-twinned gypsum (20–30 μm in size) usually occurred on the halite surface together with more soluble salts like epsomite and silvine (Figures 4c and d). Epsomite showed xenomorphic shapes filling open spaces (Figure 4d).

3.3. Pore system characterization

3.3.1. Mercury intrusion porosimetry (MIP)

MIP is a suitable technique in the analysis of the pore size distribution in the mesoporous and macroporous range on a variety of stones (Nicholson, 2001; Přikryl et al., 2003; Tuğrul, 2004) and can be also applied to relatively low porous materials like those used in this research. Figs. 5a and b (black lines) show the pore size distribution obtained by means of MIP for rough and polished samples measured before and after the ageing test respectively. Fresh rough samples display a main distribution of pores ranging from 20 to 200 μm with two maxima around 20 μm and 100 μm. The total open porosity associated with this distribution is 2.82 ± 0.33 (Table 3). In contrast, open porosity in fresh polished samples is lower (2.01 ± 0.28, Table 3) and shows only one peak at 8–10 μm (Figure 5b).

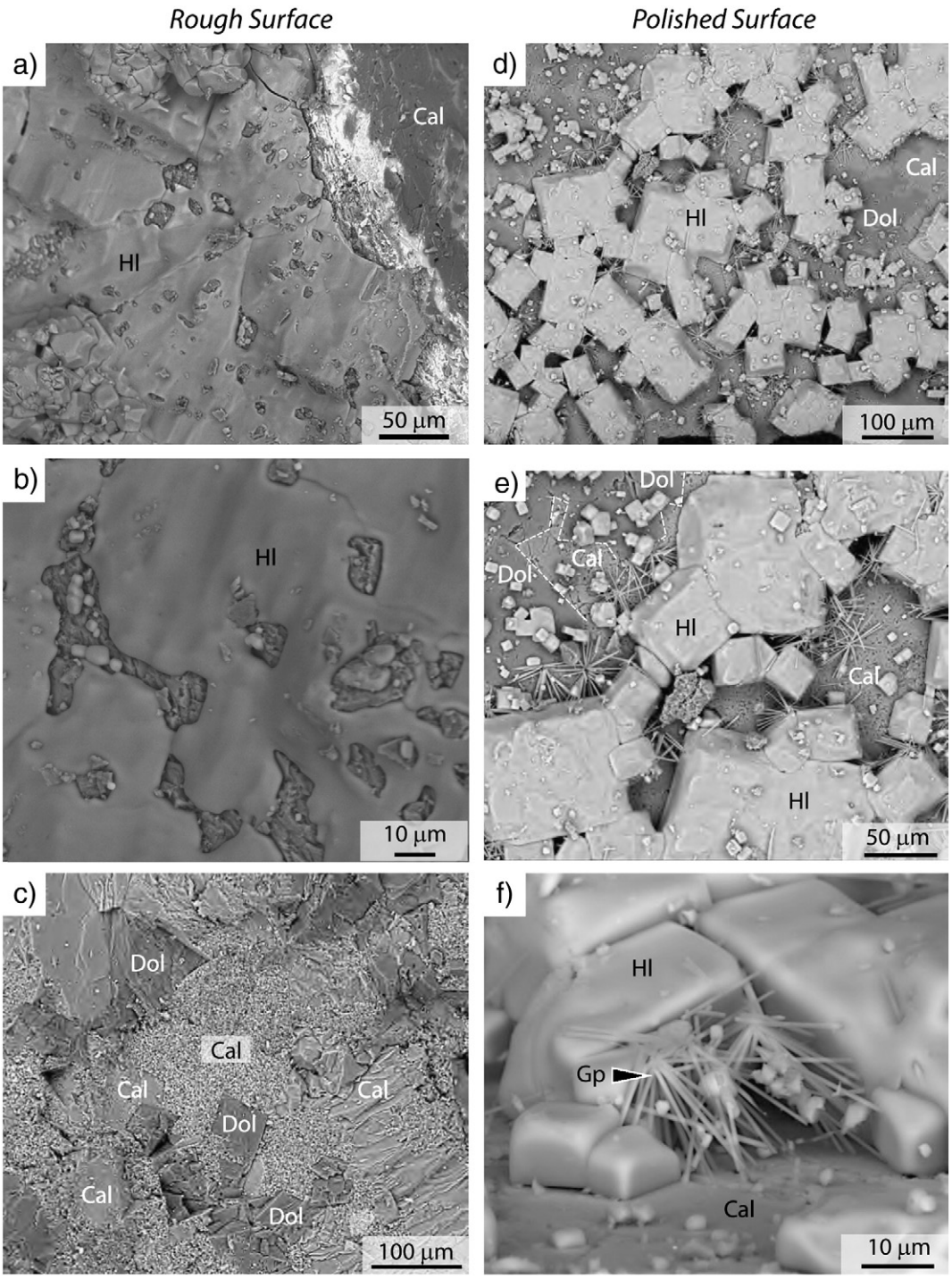

Fig. 3. Electron backscattered images taken with ESEM of the aged Sierra Elvira limestone: (a) rough surface with massive and homogeneous halite crust, (b) detail of halite crust where irregularities on the rough surface inhibited the continuity of the crust, (c) micritic calcite (center) where sparitic calcite cleavage surfaces are profusely affected by micropitting. Note that dolomite cleavage surfaces (in dark grey) are significantly less damaged, (d) polished surface covered by tabular euhedric halite and acicular gypsum crystals, (e) detail of the crust showing different degree of weathering damage of calcite and dolomite grains, (f) detail of radial aggregates of multiple aciculae gypsum crystals partially overgrown by tabular halite crystals. Cal: calcite; Dol: dolomite; Hl: halite; Gp: gypsum.

After the ageing test two cases are considered: (1) MIP measures done in the samples after the ageing test and thus potentially containing crystallized salts in their porous network and (2) MIP measures performed following limestone washing in distilled water during one week after the ageing test. Only the pore size distribution of rough samples was significantly modified in both cases when compared to the fresh samples. In the rough samples the infilling of pores after the ageing test was readily observed, where crystallizing salts resulted in a decrease of the porosity in the range of 20–100 μm (i.e. binding effect according to Cardell et al., 2008) and a slight increase for smaller pore sizes (Figure 5a, blue line) which eventually result in a slight increase in open porosity (from 2.82 ± 0.33 to 3.51 ± 0.22, Table 3). The original porosity was recovered after sample washing (Figure 5a, red line); however, in addition, significant new porosity in the range of 3–20 μm was generated. Thus, it is inferred that this new porosity was caused by the pore pressure

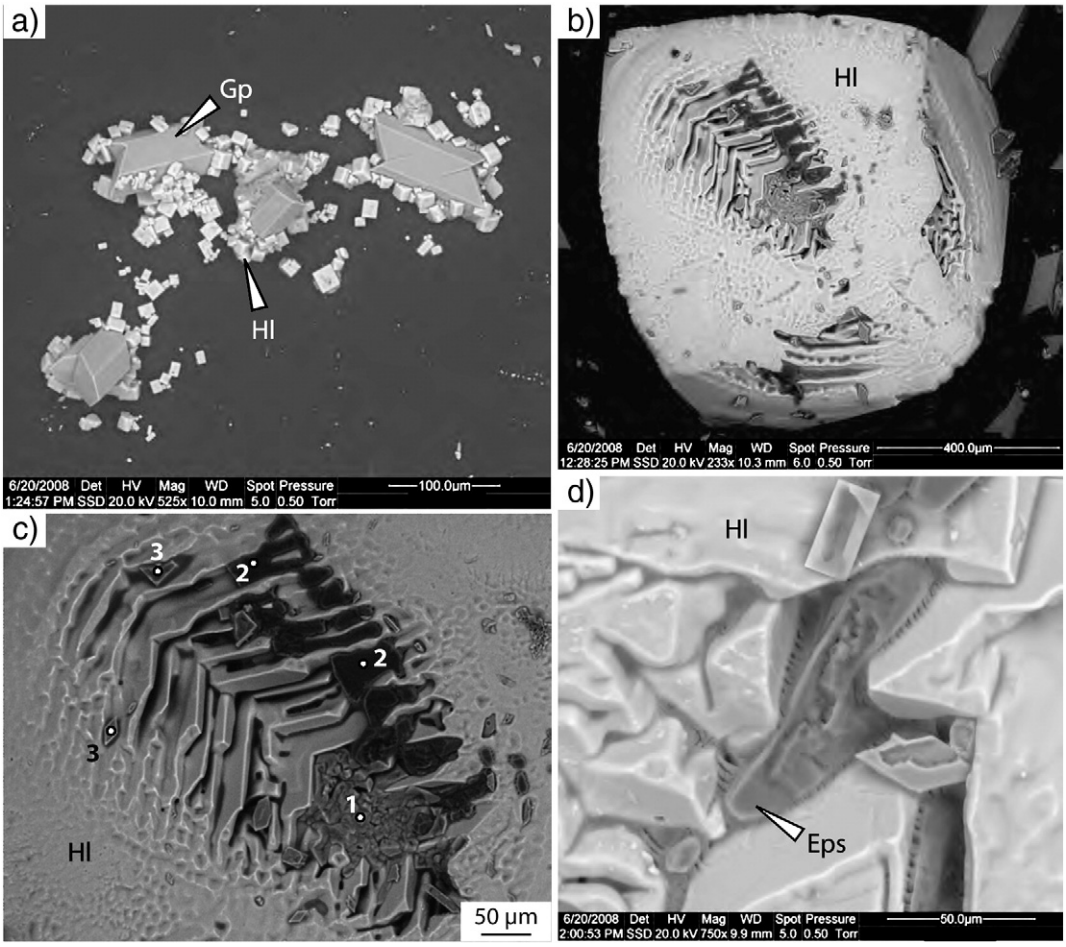

Fig. 4. Electron backscattered images of the blank crystallization test: (a) twinned gypsum (Gp) crystals partially overgrown by euhedral halite (Hl), (b) large halite crystal (ca. 800 µm) with hopper morphology, (c) enlarged area from (b) showing the occurrence of silvine-rich aggregate (1), epsomite (2) and gypsum (3) in to the hopper halite crystal, (d) detail of one xenomorphic epsomite (Eps) growing in halite boundary grains.

increase due to crystallization of salts (halite and gypsum) produced during the ageing test. Indeed, salt crystallization induced a substantial increase in the open porosity from 2.82 ± 0.33 to 5.90 ± 0.27. In contrast, polished samples only show a marginal variation in the pore system during the ageing test which results in a slight increase in the open porosity from 2.01 ± 0.28 to 3.65 ± 0.21 (Figure 5b and Table 3).

3.3.2. Argon adsorption

Porous properties for the smallest range size (microporosity, <2nm and mesoporosity, 2–50 nm) can be accurately determined by gas adsorption by measuring the amount of gas adsorbed on a solid material at different pressures (e.g. Groen et al., 2003). Moreover, by inspection of the isotherms obtained from these adsorption measurements, information regarding surface area, pore volume and pore size distribution can be obtained. In this work, argon adsorption was applied to investigate the effect of the ageing test on the mesoporosity of the near surface of SE limestone tablets (Figure 6 and Table 4). All measured isotherms are of type II (Sing et al., 1985) and indicate the non-microporous nature of these samples that is further confirmed by the very low surface area (Table 4). Representative Ar adsorption isotherms of fresh rough and polished samples are shown in Fig. 6a and b. Similarly to the MIP data, it can be observed that the polishing of the limestone surface also produced a modification of the mesoporous system (compare slopes of Figures 6a and b, empty symbols). Polished samples have lower total pore volume and smaller average pore diameter than rough samples (Table 4). Furthermore little modification can be observed after the sea-salt ageing test for polished samples (the specific surface area remained unchanged, Table 4) in contrast to the rough samples where a net change in the slope of the isotherm can be distinguished (Figures 6a and b).

Finally, the BJH plots (pore size distribution curves named after Barret–Joyner–Halenda) are almost equivalent in shape for all polished samples. Pore size distribution curves for rough aged samples are slightly displaced to lower values, in agreement with lower surface area and total pore volume (Figure 6c and Table 4). The reduction of the pore volume is attributed to the precipitation of the less soluble salts (i.e. gypsum) that remained in the smallest pores after washing.

3.4. Chromatic measurements

Chromatic parameters of all studied samples are shown in Table 5 (these are average values of three measurements for each sample and their standard deviations). Perceptible visual changes are achieved only when ΔE^* (total color difference $= \sqrt{(\Delta L^*)^2 + (\Delta a^*)^2 + (\Delta b^*)^2}$) exceeds three units. Thus color alterations were observed in all aged samples with exception of the rough ones ($\Delta E^* = 2.90$). Nevertheless, when salts were mechanically removed visual changes were perceptible in both rough and polished samples (Table 5). Indeed, luminosity increased in both rough and polished samples after mechanical cleaning until reaching similar values (L~69) (Figure 7a). However, after the mechanical elimination of the salt crusts, the ΔL^* (brightness difference) was higher in the polished samples than in the rough ones (15.44 vs. 5.11 respectively, Table 5), as can be observed in Fig. 7a.

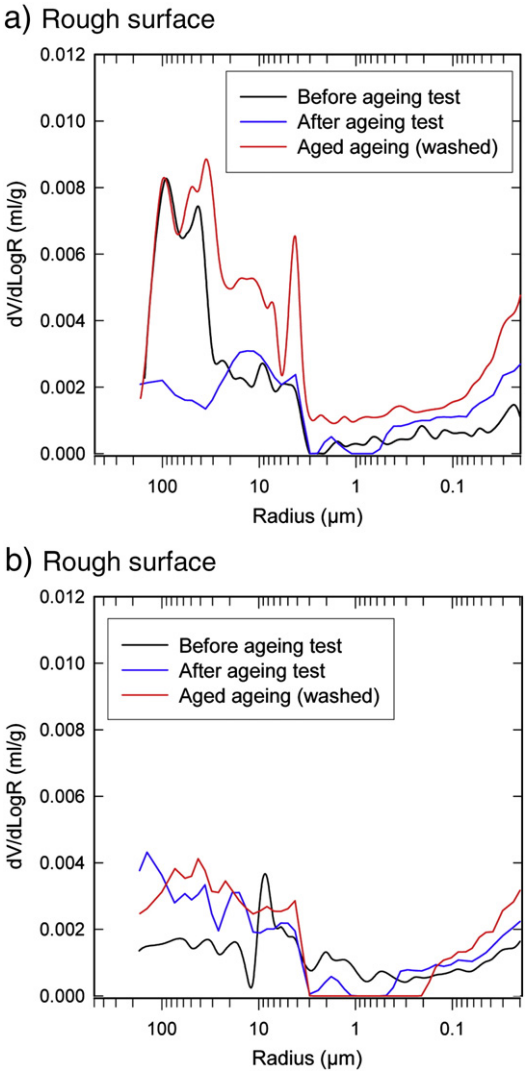

Fig. 5. Pore size distribution for rough (a) and polished (b) SE limestones before and after the test measured by mercury intrusion porosimetry (MIP). Black lines show fresh samples, blue lines aged samples, with precipitated salts and red lines aged washed samples.

On the other hand, chromatic parameter variations related to the fresh limestones can be quantified together by means of chroma differences. Fig. 7b shows an important decrease of chroma after the ageing test only for the polished surface limestones, but not for the rough surface samples that remained constant. Moreover, rough and polished samples became more blue after the test as the b* (yellow-blue) component decreased in both cases. On the contrary, the a* (red-green) component decreased only in the polished aged samples which became more green, while it increased in the rough aged samples toward more red values (Table 5).

Table 3
Mercury intrusion porosimetry parameters for SE limestone samples with rough and polished surfaces before and after the sea-salt ageing test: n_0 = open porosity (%); ρ_A = apparent (skeletal) density (g cm^{-3}); ρ_B = bulk density (g cm^{-3}).

Surface	Type	n_0	ρ_A	ρ_B
Rough	Fresh	2.82 ± 0.33	2.76 ± 0.04	2.69 ± 0.01
	Aged	3.51 ± 0.22	2.71 ± 0.02	2.61 ± 0.02
	Washed	5.90 ± 0.27	2.72 ± 0.01	2.62 ± 0.04
Polished	Fresh	2.01 ± 0.28	2.71 ± 0.01	2.67 ± 0.01
	Aged	2.65 ± 0.32	2.71 ± 0.02	2.65 ± 0.04
	Washed	3.65 ± 0.21	2.71 ± 0.02	2.62 ± 0.03

4. Discussion

4.1. Factors controlling the nature and morphology of the saline crust

All studied limestones were aged in the same salt-spray test, so they were subjected to the same sea-water spray and experimental conditions (number of cycles, distance from the spray source, temperature, humidity, etc.). Therefore, considering that the limestone mineralogy is similar, the above described contrasting salt morphologies observed in the rough and polished surfaces must be related to their surface finishing, as found in other sea-salt tested stones (Urosevic et al., 2010). In fact, the different surface micro-textures of the limestone samples involve different evaporating and water absorption conditions. Physical interaction between marine aerosol and rock substrates is complex, and the control that these interactions exert on the kinetics of salt crystallization is not fully understood, especially in large heterogeneous systems like porous stones (e.g. Theoulakis and Moropoulou, 1999; Kubik and Kucharczyk, 2008). Consequently the relation between surface roughness and salt crust morphologies (that eventually determine stone decay) is not straightforward. Our observations enable, however, to tackle more precisely this complex interrelation because of the use of the same substrate composition and microclimatic conditions. Moreover, since extreme corrosion morphologies like deep V-in-V etching or grain boundary widening reported by Thornbush and Viles (2007) were not observed, it seems that dissolution processes were minor and thus do not control the morphology of crystals in the saline crusts.

Crystal morphology reveals the phenomena controlling the process of crystal growth (Zehnder and Arnold, 1989; Theoulakis and Moropoulou, 1999; Cardell-Fernández and Rodríguez-Gordillo, 2005; Cardell et al., 2008) and therefore can be used to constrain the degree of wetting and evaporation/infiltration rate on the near stone surface (e.g. Török and Rozgonyi, 2004). As stated by Moropoulou et al. (1995) and Theoulakis and Moropoulou (1999), rounded external surfaces of halite crystals, such as those observed on our aged rough samples (Figures 3a and b), are usually formed when ion diffusion controls the growth process suggesting that moderate to low humidity prevailed during crystallization. On the contrary isometric halite crystals show their specific equilibrium form (Figures 3d and e) which indicates that crystal growth was controlled by surface reactions, thus suggesting relatively high humidity values (Arnold and Zehnder, 1989; Moropoulou et al., 1995; Theoulakis and Moropoulou, 1999; Cardell-Fernández and Rodríguez-Gordillo, 2005).

The morphology of NaCl crystals grown from aqueous solutions in a closed system is mainly controlled by different temperature gradients where both {100} and {111} hopper cubes forms can be developed (Aquilano et al., 2009). In our crystallization test, which corresponds to a closed system, small euhedral {100} forms (<40 μm in length, Figure 4a) and large {100} hopper cubes (>500 μm in length, Figure 4a) were accordingly observed. In contrast, crystals larger than 500 μm and hopper morphologies were systematically lacking in the rough and polished limestone substrate. This strongly suggests that the crystallization of halite and gypsum on the limestone took place in an open system where the saline solution was able to penetrate into the porous network below the surface. Moreover, the gradation in halite morphology and gypsum proportion of the crust is apparent from samples with rough and polished surfaces. This implies that the porosity network of polished samples is effectively less interconnected and leads to a less permeable substrate, in agreement with results from calcareous stones monuments exposed to marine environment in SW France (Cardell et al., 2003a).

The change of the gypsum proportion on the limestone surface from rough to polished samples is also noteworthy. This further suggests the higher permeability of the rough surface, which inhibits the formation of a continuous water-rich solution layer on the surface. Therefore in the case of the rough surface, the crystallization of gypsum was

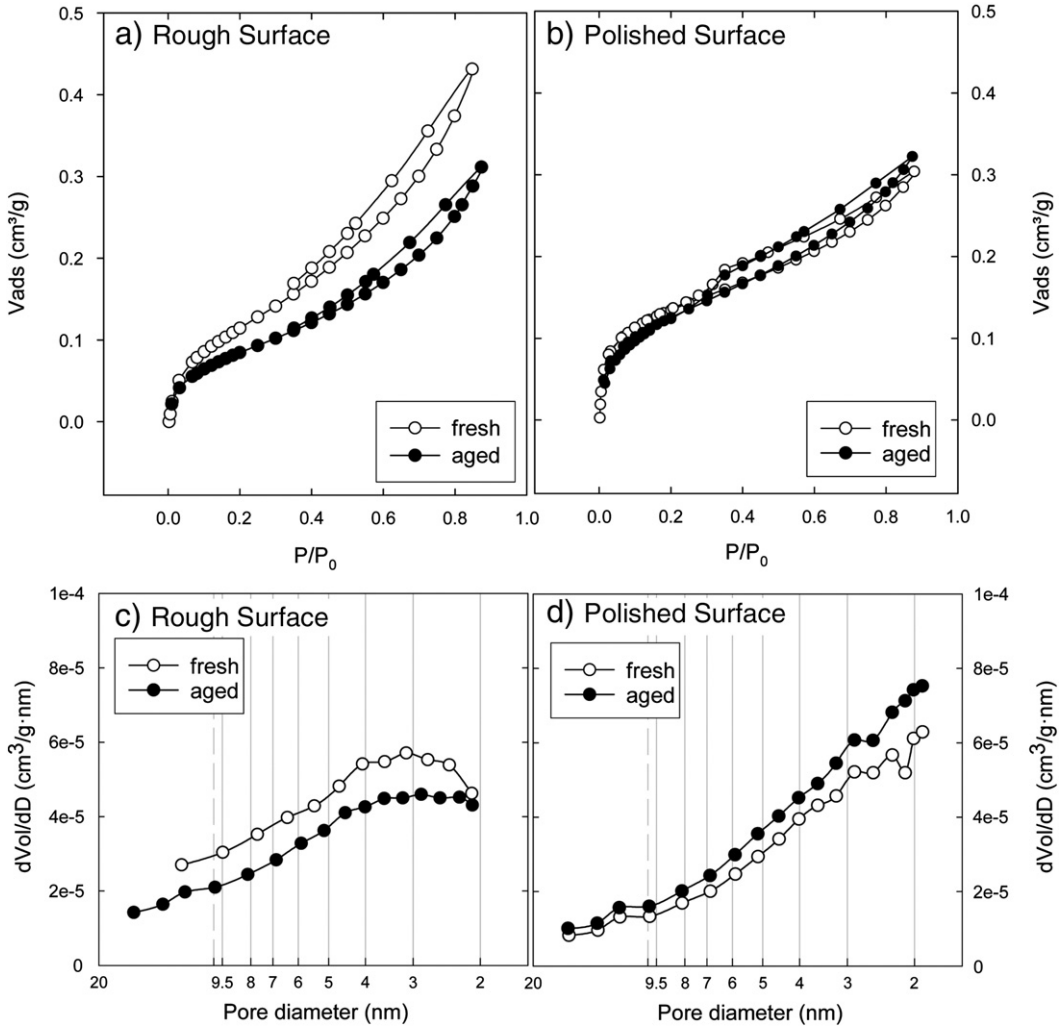

Fig. 6. Ar adsorption isotherms (−196 °C) for rough (a) and polished samples (b) before (empty symbols) and after the ageing test (black symbols). BJH pore size distribution plot for rough (c) and polished (d) samples before (empty symbol) and after the ageing test (black symbols).

enhanced in the porous network whereas in the polished samples a more wetted surface enabled gypsum crystallization with needle-like morphologies (Figures 3d-f). The occurrence of gypsum subefflorescences in the rough samples has important consequences for its decay due to salt damage as will be demonstrated later (see below). The end member of the closed system precipitation is again represented by the glass crystallizer (blank crystallization test). Here the gypsum occurs with stable equilibrium morphologies and as large crystals imposed by the impermeable nature of the substrate. It is concluded that the occurrence of these equilibrium gypsum morphologies are unlikely in nature because the requirements of a perfect impermeable substrate are not present.

In summary, the causes of the contrasting mineralogy and habits of the precipitated salts in the different substrates (rough and polished limestones and glass crystallizer) are salt solubility, substrates' microtextural characteristics and their surface pore systems. The latter influences fluid (saline solution) transport toward the substrate interior. Since the glass crystallizer can be considered a non-porous substrate, migration of the saline solution inside this material is negligible. Thus, after drying cycles the soluble salts contained in the seawater spray become concentrated by evaporation and precipitate on the surface glass substrate. Considering the ionic composition of the seawater used (Cl^-, NO_3^-, SO_4^{2-}, Ca^{2+}, K^+, Na^+ and Mg^{2+}) the resulting crystallized salts (detected with ESEM-EDS) were halite, gypsum, silvine and epsomite. Salts rich in NO_3^- were not identified, probably due to the low amount of NO_3^- in the seawater used (see Table 2).

By contrast, penetration of the saline solutions into the porous limestones depends on their surface finishing (related with their surface pore systems). The salts crystallizing onto or close to the stone surface are the most abundant salts present in the seawater used (i.e. NaCl) and the least soluble salts, namely gypsum. On the other

Table 4
Pore system characteristics determined by Ar adsorption of SE limestone samples with rough and polished surfaces before and after the ageing test.

	Fresh stone samples		Aged samples	
	Rough surface	Polished sample	Rough surface	Polished sample
Specific surface area (BET), m^2/g	0.410 ± 0.063	0.383 ± 0.024	0.266 ± 0.043	0.395 ± 0.014
Total pore volume, cm^3/g	$4.2 \pm 0.5 \times 10^{-4}$	$2.9 \pm 0.4 \times 10^{-4}$	$3.6 \pm 0.7 \times 10^{-4}$	$3.6 \pm 0.3 \times 10^{-4}$
Average pore diameter, nm	2.54 ± 0.18	2.02 ± 0.16	2.16 ± 0.16	1.91 ± 0.10

Reported values are the mean and standard deviation of 3 measurements.

Table 5
Mean values and standard deviation of chromatic parameters and their variations in tested SE limestones, before and after mechanical cleaning of salts on their surfaces.

Surface	Type	L*		a*		b*		C*		H*		ΔL*	Δa*	Δb*	ΔC*	ΔE*
		Mean	σ	Mean	σ	Mean	σ	Mean	σ	Mean	σ					
Rough	Fresh	72.67	0.69	−0.24	0.03	1.47	0.13	1.49	0.12	99.13	1.29					
	Aged	69.90	0.29	0.53	0.02	1.04	0.20	1.17	0.17	62.92	5.43	−2.77	0.77	−0.43	−0.32	2.90
	Rasped	77.78	0.61	0.41	0.08	1.18	0.22	1.25	0.23	70.89	0.96	5.11	0.65	−0.29	−0.24	5.16
Polished	Fresh	53.12	0.33	1.24	0.02	8.61	0.19	8.70	0.19	81.83	0.07					
	Aged	63.52	0.80	0.96	0.11	3.42	0.29	3.56	0.31	74.28	0.56	10.39	−0.27	−5.19	−5.14	11.62
	Rasped	68.57	1.45	1.04	0.12	5.87	0.46	5.96	0.46	79.98	0.84	15.44	−0.20	−2.74	−2.74	15.69

L* brightness; a* red-green components; b* yellow-blue components; C* chroma; H* hue; $\Delta C^* = \sqrt{(\Delta a^*)^2 + (\Delta b^*)^2}$; $\Delta E^* = \sqrt{(\Delta L^*)^2 + (\Delta a^*)^2 + (\Delta b^*)^2}$.

hand, hygroscopic and deliquescent salts like epsomite and silvine (only observed in the blank crystallization test) tend to disappear after numerous spray cycles, thus explaining their absence on the surface of salt-tested rocks due to surface washing and percolation into the porous network (Del Monte and Rossi, 1997).

All these observations clearly indicate that subtle changes in the limestone roughness due to commercial surface finishing may induce important variations in the morphology and composition of the crystallized salts. The following paragraphs discuss how these differences control the weathering pattern of the limestone surface.

4.2. Modification of the limestone pore system

It has been shown previously that the commercial finishing (i.e. polishing) results in a modification of near-surface limestone porosity by reducing the porosity and/or the interconnectivity of the porous network (Figures 5 and 6 and Table 3). This could be explained by the infilling of pores by smaller particles that result either from the abrasive used during the grinding and polishing (e.g. Erdogan, 2000) or from the disaggregation of the limestone itself during this process. Comparison of the pore systems before and after the ageing test in the studied limestones enabled evaluation of this effect on the damage induced by salt crystallization.

The reduction of the interconnectivity and open porosity due to polishing had a strong influence on the weathering behavior during the sea spray ageing test. In general the pore system of the rough surfaces was significantly modified after the ageing test whereas little modification was found in the case of the polished samples. The higher macro- and mesoporosity of the near surface in the rough samples compared to the polished ones result in a higher permeability that modified the morphology of the crystallized phases and, more importantly, induced the crystallization of soluble and insoluble mineral phases on the near surface porous network. It is interesting to point out that gypsum preferentially precipitated inside the limestone when the surface porosity was higher whereas low permeability surfaces from the polish samples enhanced gypsum crystallization on the limestone surface. It is inferred, therefore, that, in addition to halite, the site where gypsum precipitates eventually controls the higher weathering (i.e., increase in the net open porosity, Figures 5a and 6a, c) of the rough samples after the ageing test. A similar conclusion was reached by Cardell et al. (2003b) who studied the weathered granite and carbonate stone surfaces. In their study the occurrence of insoluble salts such as gypsum with needle-like morphologies was preferentially observed in low- porous granites that experienced little modification of its pore system after the ageing test (their Figure 2).

Modification of the pore system induced by salt crystallization is a well-known process in porous materials (e.g. Scherer, 1999; Angeli et al., 2008) and is especially relevant for calcarenites, porous limestones and sandstones, but is less constrained for low porous material like cemented limestones (Cardell et al., 2003b, 2008; Kramar et al., 2010b) like the studied samples. Our results show that this process is also significant in the SE limestone where development of new porous sizes and an increase of open porosity were observed in the rough samples. This observation has important implications for understanding the rock weathering in coastal areas where stone surfaces are prone to salt-decay by fog sea-salt deposition (Cardell et al., 2003a; Stefanis et al., 2009). Polishing of the stone surface would partially inhibit this effect by reducing the open porosity of the stone surface and therefore

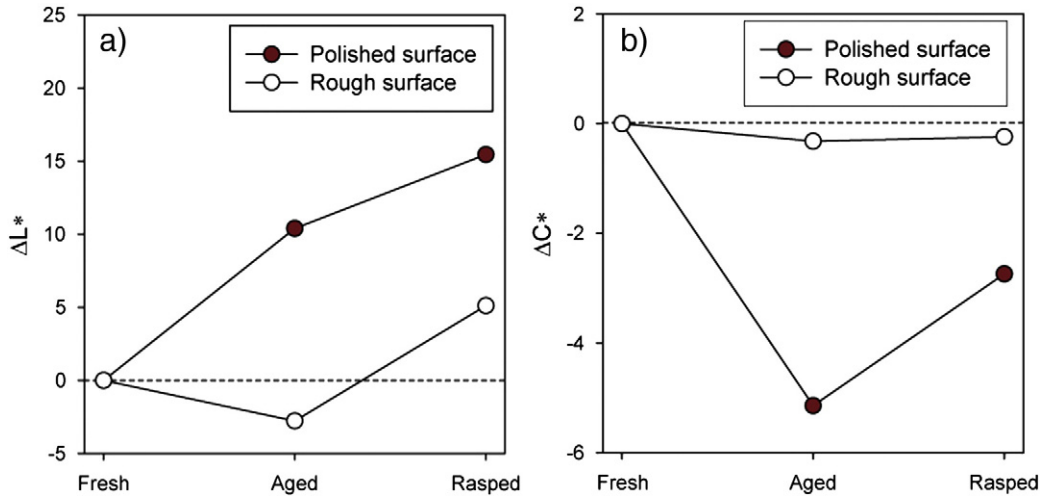

Fig. 7. Changes in the chromatic parameters of the limestone with rough (empty dots) and polished surface (filled dots) between fresh samples, aged ones and aged samples after mechanical salt cleaning: (a) variation of brightness (ΔL*) and (b) variation of chroma (ΔC*).

enhancing halite and gypsum crystallization onto the stone surface (efflorescences) which are far less aggressive than its crystallization into the pore network (subefflorescences).

4.3. Color modification due to sea spray deposition

Many processes may be responsible for chromatic changes associated with stone weathering including oxidation of chromogen minerals due to atmospheric exposition, microorganisms, black soiling or salt efflorescences (Benavente et al., 2003; Grossi et al., 2007; Urosevic et al., 2010, 2012). In the present study all chromatic changes should be attributed to salt crystallization as there is no evidence for an important chemical interaction between the stones and the sea-salt spray or iron oxidation (staining).

From the above observations it can be stated that the polished samples were less affected by the ageing test based on the minimal modification of their pore systems. On the contrary, in terms of chromatic parameters, this commercial finishing causes greater aesthetic degradation in the limestone surface compared to the weathered rough limestone. When the original surface is rough a slight decrease in luminosity and chroma are observed (Figures 7a and b) after the ageing test. The same evolution was noted by Alonso et al. (2008) in ornamental granites after 15 cycles of crystallization tests. On the contrary, polished limestone shows a considerably increase in L^* after the ageing test. The higher increase in luminosity and decrease in chroma after salt crystallization on the polished surfaces (Figures 7a and b) is explained by the intrinsic whitish color of halite and gypsum in combination with a substrate (polished limestone) which originally has lower luminosity and higher chroma than its rough equivalent (Table 5). Further increase in luminosity during the mechanical cleaning stage for both commercial finishings can be attributed to the development of salt cleavage planes and the surface reflection of the salts enhanced by the rasping procedure.

5. Conclusions

A realistic sea-salt spray test has been conducted in rough and polished surface tablets of a low-porous limestone (Sierra Elvira, SE, limestone) widely used as a building and decorative stone in Spain. Macroscopic observation revealed that no apparent stone detachments occurred during the test in any of the samples, irrespective of their surface finishing. This is attributed to the fact that SE limestone is a compact, low-porous and homogeneous rock with an interlocking crystalline texture that prevents intensive salt weathering. However a detailed analysis of the pore system modification after the sea-salt spray ageing test reveals significantly contrasting behavior between rough and polished samples. Salts precipitated as crusts in both rough and polished limestones, though with different compositions and morphologies. These results indicate that stone surface finishing strongly controlled salt spray absorption and salt crystallization onto the stone surfaces.

The porosity reduction during the polishing process of the limestone leads to variable salt damage behavior. Gypsum preferentially crystallizes in the porous system of the rough samples compared to the polished ones where needle-like gypsum aggregates are frequent at the stone surface after the ageing test. This suggest that gypsum (and halite) crystallization inside the near surface of rough samples result in the development of new pore sizes and an increase of the open porosity by coeval opening of micro-fissures of 3–20 μm. As a consequence the open porosity is doubled. On the contrary the binding effect of the commercial finishing process results in a limited modification of the pore system of the polished samples where gypsum and halite preferentially precipitate onto the stone surface.

Furthermore, this work shows that different surface finishing treatments in commercial stones not only lead to contrasting decay responses in coastal environments, but also have implications in surface color modifications attained after salt precipitation and subsequent cleaning. In this regard, after the sea-salt test all the studied limestones became more blue (cold tone) while luminosity and chroma strongly decreased, specifically in the polished samples. Thus, although polished limestones are more robust against salt induced damage they are more prone to chromatic modification by losing their valued warm tonality, which is not recovered by simple salt mechanical removal.

Acknowledgments

Financial support for this work was provided by the Andalusian Research Group RNM-179. M. Urosevic is supported by a fellowship from the Spanish Science Ministry (AP2006-036). We thank A. Kowalski for English revision. Two anonymous reviewers are thanked for their insightful comments and suggestions.

References

Alonso, F.J., Vázquez, P., Esbert, R.M., Ordaz, J., 2008. Ornamental granite durability: evaluation of damage caused by salt crystallization test. Materiales de Construcción 58, 191–201.
Angeli, M., Benavente, D., Bigas, J.-P., Menéndez, B., Hébert, R., David, C., 2008. Modification of the porous network by salt crystallization in experimentally weathered sedimentary stones. Materials and Structures 41, 1091–1108.
Angeli, M., Hébert, R., Menéndez, B., David, C., Bigas, J.P., 2010. Influence of temperature and salt concentration on the salt weathering of a sedimentary stone with sodium sulphate. Engineering Geology 115, 193–199.
Anwar Hossain, K.M., Easa, S.M., Lachemi, M., 2009. Evaluation of the effect of marine salts on urban built infrastructure. Building and Environment 44, 713–722.
Aquilano, D., Pastero, L., Bruno, M., Rubbo, M., 2009. 1 0 0 and 1 1 1 forms of the NaCl crystals coexisting in growth from pure aqueous solution. Journal of Crystal Growth 311, 399–403.
Arnold, A., Zehnder, K., 1989. Salt weathering on monuments. Proceedings of the 1st International Symposium. The Conservation of Monuments in the Mediterranean Basin, pp. 31–58.
Barrett, E.P., Joyner, L.G., Halenda, P.P., 1951. The determination of pore volume and area distributions in porous substances. I. Computations from nitrogen isotherms. Journal of the American Chemical Society 73, 373–380.
Benavente, D., Martínez-Verdú, F., Bernabéu, A., Viqueira, V., Fort, R., García del Cura, M.A., Illueca, C., Ordóñez, S., 2003. Influence of surface roughness on color changes in building stones. Color Research and Application 28 (5), 1–9.
Birginie, J., Rivas, T., Prieto, B., Auger, F., 2000. Comparación de la resistencia a la alteración por niebla salina de dos calizas utilizadas en la construcción mediante métodos ponderales, métodos acústicos y tratamiento de imágenes. Materiales de Construcción 50 (259), 27–43.
Buj, O., Gisbert, J., Franco, B., Mateos, N., Bauluz, B., 2010. Decay of the Campanile limestone used as building material in Tudela Cathedral (Navarra, Spain). Geological Society, London, Special Publications 331, 195–202.
Cardell, C., Delalieux, F., Roumpopoulos, K., Moropoulou, A., Auger, F., Van Grieken, R., 2003a. Salt-induced decay in calcareous stone monuments and buildings in a marine environment in SW France. Construction and Building Materials 17, 165–179.
Cardell, C., Rivas, T., Mosquera, M., Birginie, J., Moropoulou, A., Prieto, B., Silva, B., Van Grieken, R., 2003b. Patterns of damage in igneous and sedimentary rocks under conditions simulating sea-salt weathering. Earth Surface Processes and Landforms 28, 1–14.
Cardell, C., Benavente, D., Rodríguez-Gordillo, J., 2008. Weathering of limestone building material by mixed sulfate solutions. Characterization of stone microstructure, reaction products and decay forms. Materials Characterization 59, 1371–1385.
Cardell-Fernández, C., Rodríguez-Gordillo, J., 2005. A comparative study of calcarenite salt crystallisation and weathering in laboratory conditions and in a monument. 8th International Conference on Non Destructive Investigations and Microanalysis for the Diagnostics and Conservation of the Cultural and Environmental Heritage, Lecce (Italy).
Chabas, A., Jeannette, D., Lefevre, R.A., 2000. Crystallization and dissolution of airborne sea-salts on weathered marble in a coastal environment at Delos (Cyclades-Greece). Atmospheric Environment 34, 219–224.
Charola, A., Pühringer, J., Steiger, M., 2007. Gypsum: a review of its role in the deterioration of building materials. Environmental Geology 52 (2), 339–352.
Dabrio, C.J., Polo, D., 1985. Interpretación sedimentaria de las calizas de crinoides del Carixiense Subbético. Mediterráea. Serie de Estudios Geológicos (ISSN: 0212-4300) 4.
Del Monte, M., Rossi, P., 1997. Fog and gypsum crystals on building materials. Atmospheric Environment 31, 1637–1646.
Erdogan, M., 2000. Measurement of polished rock surface brightness by image analysis method. Engineering Geology 57 (1–2), 65–72.
Folk, R.L., 1981. The Petrology of Sedimentary Rocks. Hemphill Publishing Company, Austin, Texas.
Groen, J.C., Peffer, L.A.A., Pérez-Ramírez, J., 2003. Pore size determination in modified micro- and mesoporous materials. Pitfalls and limitations in gas adsorption data analysis. Microporous and Mesoporous Materials 60 (1-3), 1–17.

Grossi, C.M., Brimblecombe, P., Esbert, R.M., Alonso, F.J., 2007. Color changes in architectural limestones from pollution and cleaning. Color Research and Application 32 (4), 320–331.
Horemans, B., Cardell, C., László Bencs, B., Kontozova-Deutsch, V., De Wael, K., Van Grieken, R., 2011. Evaluation of airborne particles at the Alhambra monument in Granada, Spain. Microchemical Journal 99, 429–438.
Kontozova-Deutsch, V., Cardell, C., Urosevic, M., Ruiz-Agudo, E., Deutsch, F., Van Grieken, R., 2011. Characterization of indoor and outdoor atmospheric pollutants impacting architectural monuments: the case of San Jerónimo Monastery (Granada, Spain). Environmental Earth Science 63, 1433–1445.
Kramar, S., Urosevic, M., Pristacz, H., Mirtič, B., 2010a. Assessment of limestone deterioration due to salt formation by micro-Raman spectroscopy: application to architectural heritage. Journal of Raman Spectroscopy 41, 1441–1448.
Kramar, S., Mladenović, A., Urosevic, M., Mauko, A., Pristacz, H., Mirtič, B., 2010b. Deterioration of Lesno Brdo limestone on monuments (Ljubljana, Slovenia). RMZ — Materials and Geoenvironment 57, 53–73.
Kubik, J., Kucharczyk, A., 2008. Salt solution flows in walls of monumental buildings. Bauphysik 30, 426–430.
Martín Ramos, J.D., 2004. XPowder: A Software Package For Powder X-ray Diffraction Analysis. Lgl. Dep. GR 1001/04, Granada.
Meira, G.R., Andrade, C., Alonso, C., Padaratz, I.J., Borba, J.C., 2008. Modelling sea-salt transport and deposition in marine atmosphere zone — a tool for corrosion studies. Corrosion Science 50, 2724–2731.
Moropoulou, A., Theoulakis, P., Tsiourva, T., Kourteli, C., Labropoulos, K., 1995. Salt and humidity impact on porous stone masonries in marine environment. In: Druzik, J.R., Vandiver, P.B. (Eds.), Materials Issues in Art and Archaeology IV, Vol. 352. Publ. Materials Research Society, p. 893.
Nicholson, D.T., 2001. Pore properties as indicators of breakdown mechanisms in experimentally weathered limestones. Earth Surface Processes and Landforms 26 (8), 819–838.
Přikryl, R., Lokajíček, T., Svobodová, J., Weishauptová, Z., 2003. Experimental weathering of marlstone from Přednćı Kopanina (Czech Republic) — historical building stone of Prague. Building and Environment 38 (9–10), 1163–1171.
Rivas, T., Prieto, B., Silva, B., Birginie, J.M., 2003. Weathering of granitic stones by chlorides: effects of the nature of the solution on weathering morphology. Earth Surface Processes and Landforms 28, 425–436.
Rivas, T., Alvarez, E., Mosquera, M.J., Alejano, L., Taboada, J., 2010. Crystallization modifiers applied in granite desalination: the role of the stone pore structure. Construction and Building Materials 24, 766–776.
Rodriguez-Navarro, C., Doehne, E., Sebastian, E., 1999. Origins of honeycomb weathering: the role of salts and wind. Geological Society of America Bulletin 111 (8), 1250–1255.
Ruiz-Agudo, E., Mees, F., Jacobs, P., Rodriguez-Navarro, C., 2007. The role of saline solution properties on porous limestone salt weathering by magnesium and sodium sulfates. Environmental Geology 52, 269–281.
Ruiz-Agudo, E., Urosevic, M., Putnis, C.V., Rodríguez-Navarro, C., Cardell, C., Putnis, A., 2011. Ion-specific effects on the kinetics of mineral dissolution. Chemical Geology 281 (3–4), 364–371.
Scherer, G.W., 1999. Crystallization in pores. Cement and Concrete Research 29, 1347–1358.
Sebastián Pardo, E., Cultrone, G., Garibaldi, V., Rodríguez Navarro, C., de la Torre, M.J., Valverde, I., 2008. La Caliza de Sierra Elvira: comportamiento petrofísico de una piedra significativa del Patrimonio Arquitectónico Andaluz. Materiales de Construcción 58, 51–63.
Silva, Z.S.G., Simão, J.A.R., 2009. The role of salt fog on alteration of dimension stone. Construction and Building Materials 23, 3321–3327.
Silva, B., Rivas, T., García-Rodeja, E., Prieto, B., 2007. Distribution of ions of marine origin in Galicia (NW Spain) as a function of distance from the sea. Atmospheric Environment 41, 4396–4407.
Simão, J., Ruiz-Agudo, E., Rodriguez-Navarro, C., 2006. Effects of particulate matter from gasoline and diesel vehicle exhaust emissions on silicate stones sulfation. Atmospheric Environment 40, 6905–6917.
Sing, K.S.W., Everett, D.H., Haul, R.A.W., Moscou, L., Pierotti, R.A., Rouquérol, J., Siemieniewska, T., 1985. Reporting physisorption data for gas/solid systems with special reference to the determination of surface area and porosity (recommendations 1984). Pure and Applied Chemistry 57, 603–619.
Smith, B.J., Török, Á., McAlister, J.J., Megarry, Y., 2003. Observations on the factors influencing stability of building stones following contour scaling: a case study of oolitic limestones from Budapest, Hungary. Building and Environment 38, 1173–1183.
Smith, B.J., Gomez-Heras, M., Viles, H.A., 2010. Underlying issues on the selection, use and conservation of building limestone. In: limestone in the built environment: present-day challenges for the preservation of the past. Geological Society, London, Special Publications 331, 1–11.
Stefanis, N.A., Theoulakis, P., Pilinis, C., 2009. Dry deposition effect of marine aerosol to the building stone of the medieval city of Rhodes, Greece. Building and Environment 44, 260–270.
Theoulakis, P., Moropoulou, A., 1999. Salt crystal growth as weathering mechanism of porous stone on historic masonry. Journal of Porous Materials 6, 345–358.
Thornbush, M.J., Viles, H.A., 2007. Simulation of the dissolution of weathered versus unweathered limestone in carbonic acid solutions of varying strength. Earth Surface Processes and Landforms 32, 841–852.
Török, Á., 2003. Surface strength and mineralogy of weathering crusts on limestone buildings in Budapest. Building and Environment 38, 1185–1192.
Török, Á., Rozgonyi, N., 2004. Morphology and mineralogy of weathering crusts on highly porous oolitic limestones, a case study from Budapest. Environmental Geology 46, 333–349.
Tuğrul, A., 2004. The effect of weathering on pore geometry and compressive strength of selected rock types from Turkey. Engineering Geology 75 (3–4), 215–227.
UNE-EN 14147, 1994. Natural stone test methods. Determination of Resistance to Ageing by Salt Mist.Spanish Association for Standardisation and Certification (AENOR), Madrid.
Urosevic, M., Sebastian-Pardo, E., Cardell, C., 2010. Rough and polished travertine building stone decay evaluated by a marine aerosol ageing test. Construction and Building Materials 24, 1438–1448.
Urosevic, M., Yebra-Rodríguez, A., Sebastián-Pardo, E., Cardell, C., 2012. Black soiling of an architectural limestone during two-year term exposure to urban air in the city of Granada (S Spain). The Science of the Total Environment 414, 564–575.
Zaouia, N., Elwartiti, M., Baghdad, B., 2005. Superficial alteration and soluble salts in the calcarenite weathering. Case study of almohade monuments in Rabat: Morocco. Environmental Geology 48 (6), 742–747.
Zehnder, K., Arnold, A., 1989. Crystal growth in salt efflorescence. Journal of Crystal Growth 97, 513–521.
Zendri, E., Biscontin, G., Kosmidis, P., Bakolas, A., 2000. Characterization and physicochemical action of condensed water on limestone surfaces. In: Vasco, F. (Ed.), Proceedings of the 9th International Congress on Deterioration and Conservation of Stone. Elsevier Science B.V, Amsterdam, pp. 647–656.
Zendri, E., Biscontin, G., Kosmidis, P., 2001. Effects of condensed water on limestone surfaces in a marine environment. Journal of Cultural Heritage 2, 283–289.
Zezza, F., Macrì, F., 1995. Marine aerosol and stone decay. The Science of the Total Environment 167, 123–143.